Evolution Characteristics and Influence Mechanism of Binder Addition on Metallurgical Properties of Iron Carbon Agglomerates

JIWEI BAO, MANSHENG CHU, HONGTAO WANG, ZHENGGEN LIU, DONG HAN, LAIGENG CAO, JUN GUO, and ZICHUAN ZHAO

Utilization of iron carbon agglomerates (ICA) is considered to be an innovative technology to realize low carbon blast furnace (BF) ironmaking. The preparation of ICA with utilization of polyvinyl alcohol (PVA) and coal tar pitch (CTP) as binders was proposed in this study. The influence mechanisms of binder addition on the metallurgical properties of ICA were revealed. The results show that adding PVA is beneficial to improving the compressive strength of briquettes due to the chemical adsorption between the binder and the material particles. However, with the increase of PVA addition ratio from 0 to 1.0 pct, the compressive strength of ICA decreases from 2854 N to 2601 N. Meanwhile, the addition of PVA has no effect on the carbon crystallites structure of ICA and the reactivity of ICA present few changes, which are all at about 60 pct with the increase of PVA addition ratio from 0 to 1.0 pct. In addition, as the addition of CTP increases from 0 to 7 pct, the microstructure of ICA becomes dense and less porous, which can improve the compressive strength of ICA from 1639 to 3168 N. Although the reactivity of ICA is slightly reduced from 65.6 to 58.1 pct due to the development of carbon crystallites structure, it is still much higher than that of conventional metallurgical coke (30 to 35 pct). Meanwhile, the post-reaction strength is improved from 11.9 to 19.6 pct. However, as the addition amount of CTP exceeds 7 pct, the beneficial effects of CTP addition are attenuated. CTP is more suitable to be the binder of ICA, and the appropriate ratio of CTP is 7 pct.

https://doi.org/10.1007/s11663-020-01962-1

I. INTRODUCTION

THE demand for steel in China is increasing with the further development of industrialization and urbanization. As a result, energy and fuel consumption in steel industry have increased rapidly, which places a serious burden on the environment and climate, especially the greenhouse effect. The consumption of fossil fuels has produced large quantities of CO_2 greenhouse gases.[1,2] In China, the CO_2 emission from the steel industry accounts for approximately 15 pct of the whole domestic carbon dioxide emissions, and the CO_2 discharged from the BF ironmaking system accounts for about 80 pct of the total steel industry.[3–5] Moreover, with the reducing of coking coal resources in China and the rising price of coking coal, the development and utilization of non-coking coal will be of great significance.[6] Therefore, the BF ironmaking is facing the double pressures of high-quality resources shortage and carbon emission reduction in China, and it is urgent to develop the cutting-edge technology of low carbon BF ironmaking. Iron coke (or iron carbon agglomerates ICA) is one of the core technologies of low carbon BF ironmaking.

As an innovative technology of low carbon BF ironmaking, iron coke has attracted more and more attentions. Iron coke is a carbon iron composite material with high reactivity. The raw material source of iron coke can be weak caking and non-caking coals, which greatly expands the raw material source and reduces the production cost. It was proposed by Naito *et al.*[7–10] that the utilization of highly reactive coke (carbon iron composite CIC, iron coke or ferro-coke) was considered to be an effective countermeasure to realize low carbon BF through decreasing the temperature of thermal reserve zone. It is generally believed

JIWEI BAO, ZHENGGEN LIU, DONG HAN, LAIGENG CAO, JUN GUO, and ZICHUAN ZHAO are with the School of Metallurgy, Northeastern University, Shenyang 110819, People's Republic of China. MANSHENG CHU is with the State Key Laboratory of Rolling and Automation, Northeastern University, Shenyang 110819, People's Republic of China. Contact e-mail: chums@smm.neu.edu.cn HONGTAO WANG is with the School of Metallurgy Engineering, Anhui University of Technology, Ma'anshan 243032, People's Republic of China. Contact e-mail: wanght@ahut.edu.cn

Manuscript submitted March 24, 2019.
Article published online September 28, 2020.

that the temperature of thermal reserve zone in BF is mainly determined by the starting temperature of coke gasification reaction.[11] Highly reactive iron coke can reduce the temperature of thermal reserve zone, which leads to an increase in the difference between the actual concentration and the equilibrium concentration of CO in the BF gas. As a result, the reduction driving force of iron oxide inside the BF is improved. The partial replacement of traditional coke with highly reactive iron coke in BF can improve the reaction efficiency of BF, and reduce the fuel ratio and CO_2 emission.[7–10]

Nowadays, the preparation process of iron coke mainly includes traditional coke oven process and briquetting-shaft process. In terms of the former process, the furnace wall of carbonization chamber is easily eroded by wustite from iron ore, so the temperature of coke oven is difficult to be controlled accurately. Moreover, the coking time is prolonged since the iron ore added, and the carbonization product is easily broken and oxidized by wet quenching. Wang *et al*.[12–14] prepared iron coke by hot briquetting the mixture of iron ore and coal without using binder, and found that the mechanical strength of the briquettes can be notably enhanced. Simultaneously, the mechanical strength of iron coke can be optimized by reasonably adjusting the ratio of coal and iron ore. However, the hot briquetting temperature is relatively high. Anyashiki *et al*.[15] investigated the preparation of ferro-coke by briquetting-shaft process with using two conventional binders, namely soft pitch (SOP) and asphalt pitch (ASP). It was showed that the drum index (ID_{16}^{600}) of briquettes can reach 85 pct, and the drum index (DI_{6}^{150}) of ferro-coke is up to 60 pct with adding 2 pct ASP and 3 pct SOP. In addition, Sekine *et al*.[16] studied the mixed structure of coals with binder HPC (hyper-coal, produced by solvent extraction and continuous drying of coal) under different coking conditions by Raman spectroscopy and intensity index. It was showed that a strong carbonaceous structure with high crystallinity is produced by the mutual melting of HPC and coals.

Although many studies have been done on the preparation and metallurgical properties of iron coke, there are few studies on the preparation of ICA using different binders and the influence mechanisms of binder addition on the metallurgical properties of ICA. Polyvinyl alcohol (PVA) and coal tar pitch (CTP) are often used as the binder of formcokes. This study was focused on the influencing mechanisms on the metallurgical properties of ICA with adding the binders of PVA and CTP. Firstly, the ICA was produced through briquetting by roller and carbonizing process based on Chinese raw material conditions. Secondly, the evolution characteristics for the metallurgical properties of ICA with utilizing PVA and CTP were detailedly illuminated. Finally, the interaction mechanisms inside the ICA were revealed through analyzing the microstructure, pore structure, carbon crystallites structure and functional groups by means of Scanning Electron Microscope-Energy Dispersive X-ray Spectroscopy (SEM-EDS, Zeiss, Ultra Plus), Raman spectrometer (Horiba Jobin Yvon, HR800 type, France) and Fourier transform infrared spectrometer (FTIR, Bruker, VERTEX70 type). This study could promote the practical application of ICA and make the progress of low carbon BF ironmaking technology.

II. EXPERIMENTAL

A. *Preparation of Samples*

One type of iron ore and three types of coals used in the experiment were all obtained from the HBIS Group Shisteel Company in China. The chemical composition of iron ore is listed in Table I. The total iron content and the FeO content of iron ore are approximately 65.36 and 21.86 pct. The characteristic analyses of the coals are listed in Table II. Among them, coal A is a caking coal with high volatile content and caking index, Coal B is a slightly caking coal, and coal C is a non-caking coal with higher fixed carbon and lower volatile matter. In terms of iron ore size, the particles with less than 75 μm accounts for approximately 80 pct. All the coals are crushed and screened to less than 4 mm. In addition, PVA and CTP are used as binders for the preparation of ICA. PVA is a high polymer binder, which has the characteristics of low dosage and strong bonding ability. However, such binder has few coking components and poor thermal stability. Meanwhile, CTP is an asphalt binder, which is similar to coal in structure and properties, and has a strong affinity with coal and can well infiltrate coal particles. The chemical composition of CTP is listed in Table III.

The preparation process of ICA is shown in Figure 1. Firstly, iron ore, coals and binder were thoroughly mixed in a certain proportion to get the mixtures. According to previous studies, the ratio of iron ore, coal A, coal B and coal C in the mixture was fixed at 30:45:20:5. After that, 6 pct water was added into the mixture to make PVA dissolve in water and play a binding role when PVA is used as binder, and the mixtures were immediately pressed into briquettes by roller briquetting equipment (Luoyang Kaizheng environmental protection equipment Co., Ltd, KYS175 type) under a linear pressure of 29.4 KN cm^{-1}. When CTP is used as binder, it needed to be broken to less than 1 mm in order to mix well with the raw material mixture, and the mixtures were quickly loaded into the roller briquetting machine and heated while stirring. When the mixtures were heated to 150 °C, the mixtures were pressed into briquettes by roller briquetting equipment under a linear pressure of 29.4 KN cm^{-1}.

Finally, the briquettes were carbonized using SX_2-8-13 type electric heating furnace developed by Shenyang energy saving electric furnace factory. The maximum temperature of this equipment is 1300 °C, and the molybdenum silicide rods are used as the heating elements. The briquettes were heated to 1000 °C at a heating rate of 3 °C min^{-1}, and the temperature was maintained at this level for 4 hours. The carbonized product was cooled in an inert atmosphere, and the metallurgical properties of briquettes and ICA were tested. Moreover, the external morphologies of the

produced briquettes and ICA are shown in Figure 2, and the external size of the briquettes and ICA are 31.8 × 26.6 × 17.3 and 28.4 × 24.1 × 15.8 mm, respectively. In this paper, the effects of the additive amount of binder PVA and CTP on the metallurgical properties of ICA were studied. According to the related studies about briquette and formed coke,[17–20] the amount of PVA added is generally 0.4 to 1.2 pct, and the amount of asphalt binder added is generally 5 to 15 pct. Therefore, in this paper, the addition amount of PVA is determined in the range of 0 to 1.0 pct, and the addition amount of CTP is determined in the range of 0 to 11 pct. Furthermore, ICA products with PVA and CTP binders were denoted as PVA-r and CTP-r, respectively, where r represents the addition ratios of binder.

B. *Method for the Determination of Metallurgical Properties of ICA*

The briquettes and ICA should have good mechanical strength as a feed material for blast furnaces. The compressive strength is one of the most important mechanical strength indices. For the briquettes and ICA, the compressive strength was measured by an electronic universal testing machine (WDW-QT10 type). Twelve samples were randomly selected to measure the compressive strength, and the final experimental value is the average of the remaining results after removing the maximum and minimum. In addition, the reactivity and post-reaction strength test of ICA were carried out according to the method of GB/T 4000-2017.[21] In N_2 atmosphere with flow rate of 0.8 L min^{-1} (linear velocity of 0.003 m s^{-1}). Approximately 200 g ICA are heated to 1100 °C at a rate of 10 °C min^{-1}, and then react with CO_2 (flow rate of 5 L min^{-1}, linear velocity of 0.017 m s^{-1}) for 2 hours at 1100 °C. After the reaction, the post-reaction strength of reacted ICA is performed by 600 revolutions (20 rpm × 30 min) in the I-type drum (Φ130 × L700 mm). After the drum test, the samples are screened with a 10-mm round hole sieve and the quality of the material on the sieve is recorded. The reactivity index of ICA is evaluated by the carbon conversion ratio, which is calculated by Eq. [1]. The post-reaction strength of ICA is estimated by the

Table I. Chemical Composition of Iron Ore (Weight Percent)

TFe	FeO	CaO	SiO_2	MgO	Al_2O_3
65.36	21.86	0.17	6.35	0.45	0.45

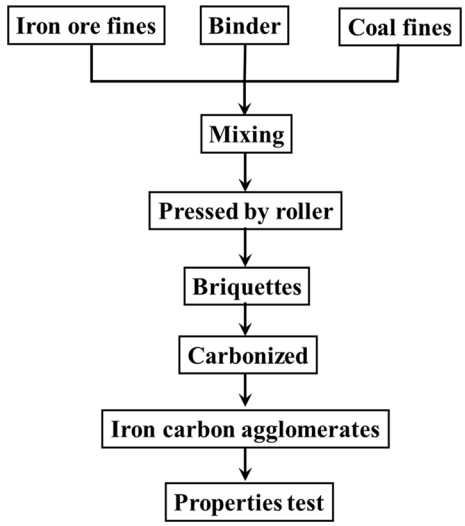

Fig. 1—Preparation process of ICA.

Table II. Characteristic Analyses of the Coals (Weight Percent, Air Dry Basis)

Coal	Fixed Carbon (Percent)	Ash (Percent)	Volatile Matter (Percent)	Chemical Composition of Ash (Weight Percent)				Caking Index (G/Percent)	Thickness of Adhesive Layer (Y/mm)
				CaO	SiO_2	MgO	Al_2O_3		
A	61.21	8.96	29.08	4.02	49.78	0.78	38.84	74	15.0
B	76.50	9.90	13.16	2.12	49.29	0.40	37.37	15	n.a.
C	78.25	13.36	7.30	3.59	50.30	1.42	35.70	n.a.	n.a.

n.a. no data available.

Table III. Chemical Composition of CTP (Weight Percent, Air Dry Basis)

Proximate Analysis						
Fixed Carbon	Volatile Matter	Ash	Moisture	S	Coking Value (Percent)	Softening point(°C)
33.21	65	0.59	1.2	0.4	48	131

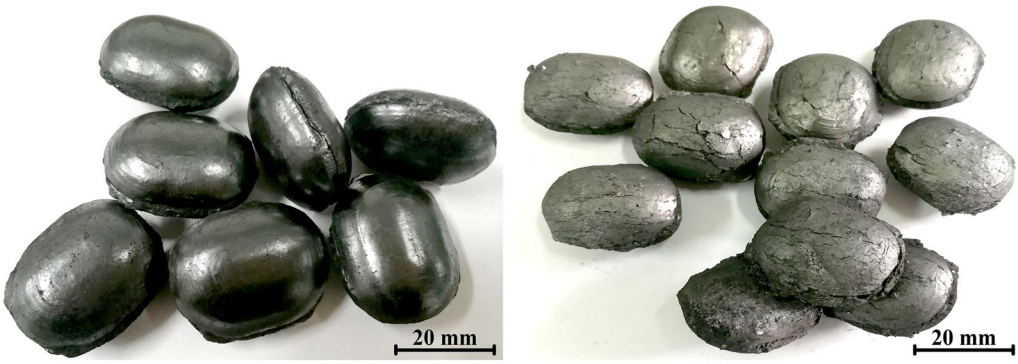

Fig. 2—External morphologies of the briquettes and ICA, (*a*) briquettes, (*b*) ICA.

percentage of the mass of reacted ICA with a particle size greater than 10 mm after the drum test to the mass of reacted ICA, as seen in Eq. [2].

$$\text{Reactivity} = \frac{m_0 \times c_0 - m_1 \times c_1}{m_0 \times c_0} \times 100 \text{ pct}, \qquad [1]$$

where, m_0 and m_1 are the mass of ICA before and after reaction, respectively, g; c_0 is the carbon content of ICA before the reaction and c_1 is the carbon content of ICA after the reaction, pct.

$$\text{Post - reaction strength} = \frac{m_2}{m_1} \times 100 \text{ pct}, \qquad [2]$$

where, m_2 is the mass of reacted ICA with the particle size larger than 10 mm after the drum test, g.

C. *Characterization Methods*

The microstructures of ICA with adding different binders were analyzed by the SEM-EDS. The samples were cut, and then the cut samples without mounting processing were ground by different grades of sandpaper and polished by a polishing machine. Finally, the surface of the sample was coated with gold-palladium alloy for SEM-EDS analysis.

Raman spectroscopy measurements were recorded at room temperature using a Horiba Jobin Yvon, HR800 type spectrometer, visible light is adopted as excitation light source, and the wavelength of excitation line is 633 nm. The spectral scanning range is 800 to 2000 cm^{-1}. The samples were scattered on glass slides for the spectral data collection.

The FTIR spectra of samples were performed at room temperature on a FTIR Spectrometer. The treated sample was mixed with pure KBr in a ratio of 1:100 and the mixtures were ground in an agate mortar for about 5 minutes to ensure adequate mixing, and then 100 mg mixtures were poured into a tablet press and pressed into thin spectral films. The thin spectral films were put into the sample room for infrared spectrum scanning test. The scanning range is 4000 to 400 cm^{-1}, and the spectral resolution is 4 cm^{-1}.

III. RESULTS AND DISCUSSION

A. *Influence Mechanism of PVA Binder on the Metallurgical Properties of ICA*

1. *Metallurgical properties of ICA*

When PVA is used as binder, it needs to be dissolved in water to play a bonding role, because PVA has good fluidity only when it is dissolved in water, and water can play a lubricating role between raw material particles and binder. In this way, PVA binder and raw material particles can be mixed evenly, and the mechanical strengths of briquettes and ICA can be improved. According to the previous research, 6 pct of moisture was the best when PVA was used as binder in the preparation of ICA. Therefore, when the amount of PVA varied from 0 to 1.0 pct, the moisture content was kept at 6 pct. The effects of PVA addition ratios on the metallurgical properties of ICA are shown in Figure 3. With the increase of PVA addition ratio from 0 to 1.0 pct, the compressive strength of briquettes is gradually increased from 417 to 716 N, but the compressive strength of ICA is decreased slightly from 2854 to 2601 N, which remains higher than 2500 N required by conventional metallurgical cokes. The addition of PVA thus, improves the compressive strength of briquettes but reduces the compressive strength of ICA. In addition, as shown in Figure 3, the reactivity and post-reaction strength of ICA are not changed significantly with the increase of PVA contents. However, the reactivity of ICA is still at a high level of around 60 pct due to the catalytic action of the formed iron (much higher than 30 pct generally required of conventional metallurgical cokes), while the post-reaction strength of ICA is about 16.5 pct.

2. *Microstructure analysis*

The mechanical strength and reactivity of ICA are generally determined by microstructure, pore structure, carbon crystallites structure and mineral composition. In order to reveal the evolution mechanism of mechanical strength and reactivity of ICA, the microstructure and pore structure of ICA with different PVA content were analyzed. Figure 4 shows the SEM-EDS analysis

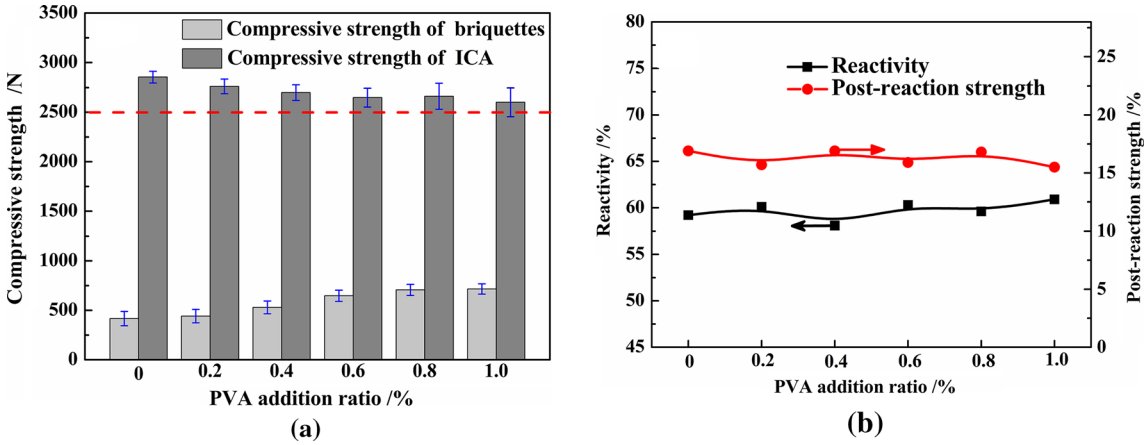

Fig. 3—Effects of PVA addition ratios on the metallurgical properties of ICA, (*a*) compressive strengths of briquettes and ICA, (*b*) reactivity and post-reaction strength of ICA.

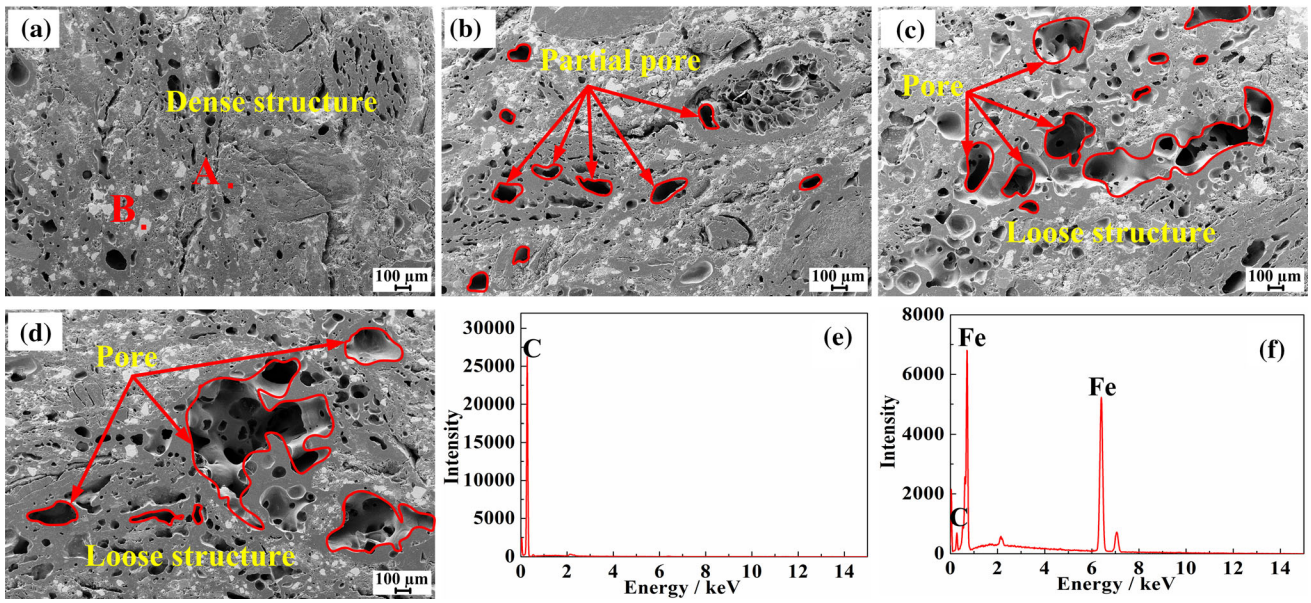

Fig. 4—SEM-EDS analysis of ICA with different PVA contents, (*a*) without adding PVA, (*b*) 0.4 pct, (*c*) 0.6 pct, (*d*) 0.8 pct, (*e*) EDS of point A, (*f*) EDS of point B.

of ICA with different PVA contents. With the increase of PVA content, the porosity of ICA gradually increases and small pores gradually grow and merge into larger pores, and the microstructure of ICA is gradually degraded and becomes loose. This is because the molecular chain of PVA is easily decomposed into small molecule volatiles such as acetic acid, acetaldehyde, butenol and water in the carbonization process, which could destroy the structure of ICA. The degradation of microstructure is the main reason for the decrease of compressive strength of ICA. However, as shown in Figure 3, the deterioration for the compressive strength ICA is not obvious due to the small amount of PVA, and the compressive strength of ICA is still at a high level.

As shown in Figure 4, the EDS analysis of ICA shows that the gray area at point A is the carbon matrix, and the white area at point B is the metallic iron, which is evenly distributed in the carbon matrix and plays a catalytic role in the gasification reaction of carbon. Therefore, the reactivity of ICA is at a high level. However, in this study, the ratio of iron ore is fixed at 30 pct, and its catalytic effect is consistent. In addition, the number of pores in ICA is increased slightly with the increase of PVA content, which has beneficial effect on the diffusion of the CO_2 gas for the gasification reaction and improving the reactivity of ICA. However, other factors should be considered, especially the carbon crystallites structure, which determines the reactivity of carbon.

3. *Raman spectra analysis*

The mechanical strength and reactivity of ICA are also closely related to the carbon crystallites structure. Raman spectra are widely used to characterize the ordered and disordered graphite structures in carbonaceous materials,[22–25] and the Raman spectra parameters can reflect the carbon crystallites structure and activity of the sample. The Raman spectra and Raman parameters of ICA with different PVA contents are shown in Figure 5. The spectra show that two major bands appear. The peak width of these two peaks is relatively large, indicating that there are other peaks. Relevant studies show that four Lorentzian bands (G, D1, D2, and D4) and one Gaussian band (D3) are most suitable for the Raman spectra of coke samples.[26–29] Therefore, the Raman spectra of ICA within the range of 800 to 2000 cm^{-1} were curve-fitted into five bands (D1, D2, D3, D4 and G). The G band (~ 1580 cm^{-1}) is considered to be the ideal graphitic lattice (E_{2g} symmetric) stretching mode [30–32]. The D1 band (~ 1350 cm^{-1}) is thought to be a typical representative of disordered graphitic lattice (graphene layer edges, A_{1g} symmetry).[30–32] The D2 band (~ 1620 cm^{-1}) is attributed to the disordered graphitic lattice (surface graphene layers, E_{2g} symmetry).[30–32] The D3 band (~ 1500 cm^{-1}) is the signal intensity between the two main peaks, derived from the amorphous carbon component.[30–32] The D4 band (~ 1200 cm^{-1}) is related to the disordered graphite lattice (A_{1g} symmetry).[30–32] The parameter I_{D1}/I_G represents the degree of graphite structure in the graphite layer. The parameter I_G/I_{all} represents the content of graphite structures. The lower the ratio of I_{D1}/I_G and the higher the ratio of I_G/I_{all} are, the higher graphitization degree of the sample is, and the lower the gasification reactivity of the carbonaceous materials is. The parameter L_a represents the carbon crystallite size. The larger L_a is, the more complete the carbon crystallites structure of the sample is. L_a can be calculated by Eqs. [3] and [4].[32]

$$L_a = C(\lambda_L)(I_{D1}/I_G)^{-1} \quad [3]$$

$$C(\lambda_L) = C_0 + \lambda_L C_1 \quad [4]$$

where $C(\lambda_L)$ is the wavelength pre-factor, and I_{D1} and I_G are the intensity of the D_1 and G bands. $C(\lambda_L)$ can be calculated by Eq. [4] when the range of wavelength is 400 to 700 nm, $C_0 = -12.6$ nm and $C_1 = 0.033$.

The higher graphitization degree of ICA indicates that the more regular arrangement of carbon crystallites structure inside ICA, which can reduce the gasification reactivity of carbon inside ICA with CO_2, The parameters I_{D1}/I_G, I_G/I_{all} and L_a of ICA with different PVA contents are shown in Figure 5. With the increase of PVA addition, the I_{D1}/I_G, I_G/I_{all} and L_a of ICA have no obvious changes, which indicates that the carbon crystallites structure of ICA is not changed significantly and there is no significant change of carbon activity in ICA. The carbon crystallites parameters of ICA showed an obviously corresponding relationship and consistent changing trend with the reactivity of ICA. Therefore, from the perspective of carbon crystallites structure, the addition of PVA has no significant impact on the reactivity of ICA. The main reason for this result is that PVA does not contain coking components. In the carbonization process of briquettes, PVA is basically pyrolyzed and volatilized, which does not participate in the construction of carbon crystallites structure in ICA. Although the addition of PVA can destroy the microstructure of ICA and provide good gas diffusion conditions for the gasification reaction of carbon, the activity of carbon crystal plays a major role in the gasification reaction. Under the condition that PVA has no significant effect on the carbon crystallites structure of ICA, the gasification reactivity of ICA has no significant change.

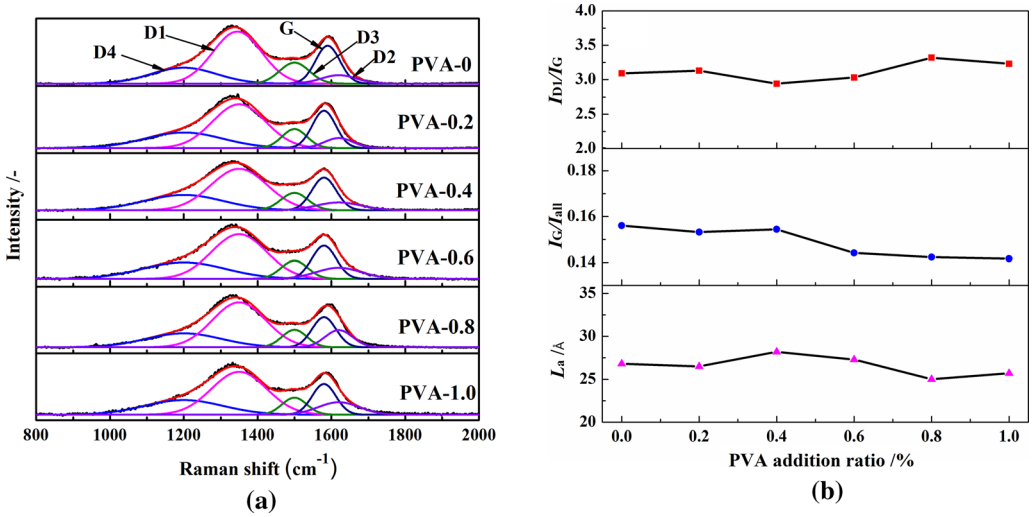

Fig. 5—(*a*) Raman spectra and (*b*) Raman parameters of ICA with different PVA contents.

The regular arrangement of carbon crystallites structure is conducive to improve the mechanical strength of ICA. According to the Raman analysis results in Figure 5, the addition of PVA does not affect the carbon crystallites structure of ICA. Therefore, from the perspective of crystal structure, PVA has no effect on the compressive strength of ICA. However, under the influence of poor thermal stability of PVA on the microstructure of ICA, The structure of ICA is damaged, and the compressive strength of ICA is slightly reduced.

4. *FTIR analysis*

FTIR is widely applied to directly detect the chemical structures of the material. In order to further reveal the influence of PVA addition on the chemical structures of ICA, the FTIR spectra of raw materials and ICA products were analyzed. FTIR spectra of the iron ore, coals (45 pct coal A, 20 pct coal B and 5 pct coal C), PVA and ICA with different PVA additions were recorded in the range of 4000 to 400 cm^{-1} as shown in Figure 6. The band assignments of FTIR spectra are listed in Table IV.[34,35] As shown in Figure 6(a), the functional groups of -OH, Si-O and Fe-O are mainly observed in the FTIR spectrum of iron ore.[33,36] For the FTIR spectrum of coals shown in Figure 6(b), the stretching vibrational modes of -OH groups are observed at 3688 and 3618 cm^{-1}. Asymmetry and symmetry stretching vibrational modes of $-CH_2$ are observed at 2918 and 2854 cm^{-1}, respectively.[37–39] The bands of 1599 and 1439 cm^{-1} are observed which are assigned to aromatic C=C stretching vibrational modes.[37–39] The appearance of the band at 750 cm^{-1} can be ascribed to the aromatic Car-H stretching vibrational.[37–39] The bands of 1730 and 1032 cm^{-1} are considered to be groups of carboxyl acids -COOH and alkyl ethers C-O, respectively.[37–39] Figure 6(c) presents the FTIR spectrum of PVA and the polar functional groups of -OH, -COOH and C-O are observed at 3425, 1736, 1258 and 1138 cm^{-1}.[40]

When using PVA as binder for the preparation of ICA, a large number of polar functional groups of -OH, -COOH and C-O in PVA molecules can form covalent bonds or ionic bonds with oxygen-containing functional groups of coals and ions of iron ore, resulting in chemical adsorption. Moreover, it is easy to form hydrogen bonds with water molecules to adsorb water molecules. PVA polymers can form irregular network structures and close connections between material particles through this chemical adsorption and cross-linking. Therefore, with the increase of PVA addition, the compressive strength of briquettes is gradually

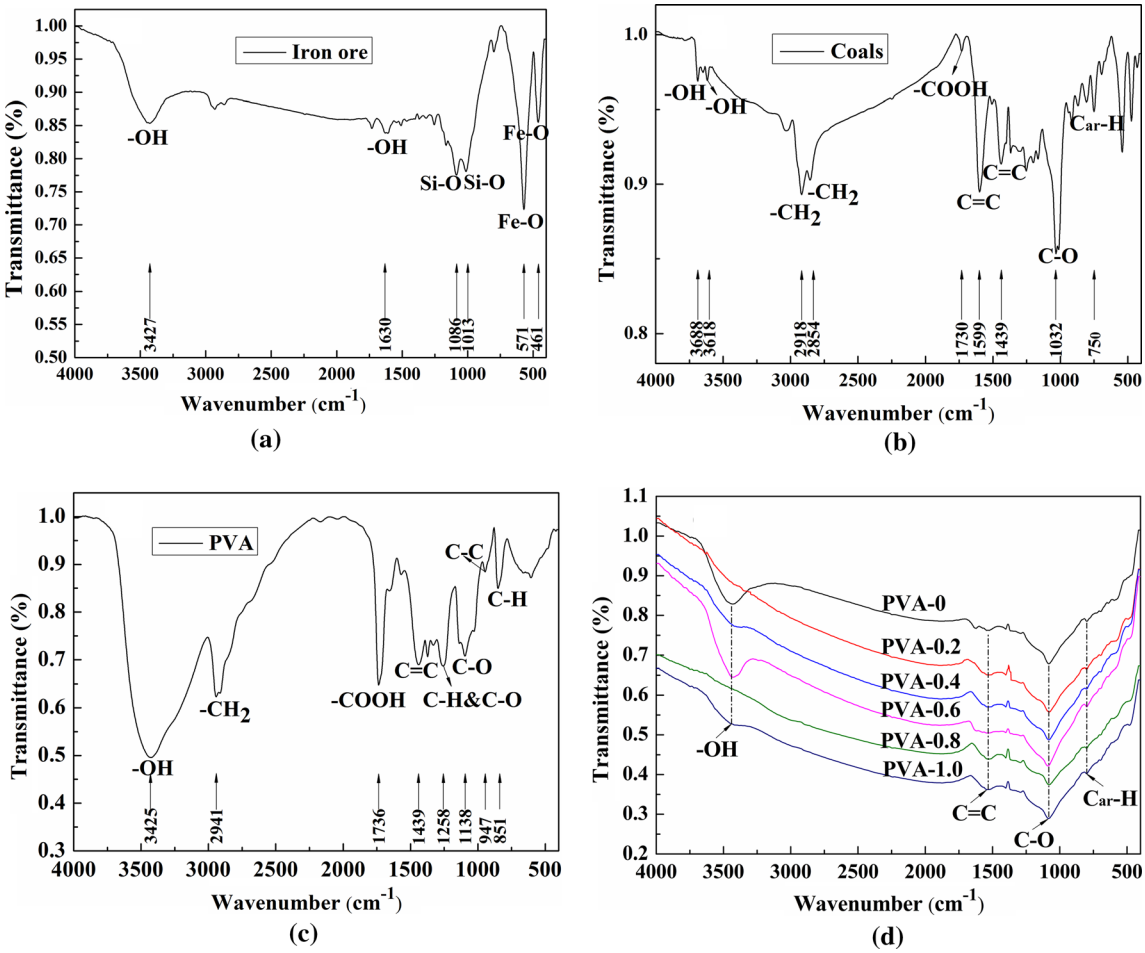

Fig. 6—FTIR spectra of (*a*) iron ore, (*b*) coals (45 pct coal A, 20 pct coal B and 5 pct coal C), (*c*) PVA, (*d*) ICA with different PVA additions.

increased. Meanwhile, the oxygen-containing functional groups and alkyl side chain of coals after carbonization at 1000 °C are almost removed. Hence, as seen in Figure 6(d), only a small amount of oxygen-containing groups (-OH and C-O) and the aromatic structure (C = C and Car-H) are left in ICA. In addition, the peak strengths of aromatic structure C = C and Car-H in ICA are not changed significantly with the increase of PVA content, which indicates that the carbon crystallites structure is changed indistinctively and there is no significant change for the activity of carbon inside ICA. The results are consistent with the previous analysis, so the addition of PVA has no obvious influence on the reactivity of ICA.

B. *Influence Mechanism of CTP Binder on the Metallurgical Properties of ICA*

1. *Metallurgical properties of ICA*

The evolution of the metallurgical properties of ICA with adding CTP is shown in Figure 7. The compressive strength of briquettes and ICA are firstly increased and then decreased with the ratio of CTP increasing from 0 to 11 pct. Meanwhile, the reactivity of ICA is firstly decreased and then increased, while the post-reaction strength shows an opposite trend to the reactivity. Furthermore, when the addition amount of CTP is 7 pct, the compressive strength of briquettes achieve higher value of around 677 N, and the compressive strength, reactivity, and post-reaction strength of ICA are all at a relatively high level of 3168 N (much higher than 2500 N required by conventional metallurgical cokes), 58.7 pct (much higher than 30 pct generally required of conventional metallurgical cokes), and 19.6 pct, respectively.

In addition, according to Figures 3 and 7, the metallurgical properties of briquette and ICA with 0 pct PVA are different from those of briquette and ICA with 0 pct CTP. The main reason is that 6 pct of moisture was still added in the preparation of ICA without PVA in order to keep consistent with the preparation conditions of ICA with other PVA ratios. In binderless molding, the strength of briquette mainly comes from the mechanical meshing force between the particles. Proper moisture can wrap and wet the coal particles, reduce the friction force, and form a liquid bridge force between the particles. Therefore, the compressive strengths of briquettes and ICA with 0 pct PVA are higher than those of briquettes and ICA with 0 pct CTP. The higher mechanical strength indicates a more compact structure, which will hinder the gas diffusion in the gasification reaction and reduce the reactivity of ICA. Therefore, the reactivity of ICA with 0 pct PVA is lower than that of ICA with 0 pct CTP.

2. *Microstructure analysis*

In order to reveal the evolution mechanism of metallurgical properties of ICA, the microstructure and pore structure of ICA with different CTP content were analyzed. Figure 8 gives the SEM analysis of ICA with different CTP contents. As the addition amount of CTP is increased to 7 pct, the porosity of ICA is gradually decreased and the microstructure of ICA becomes denser. It is because that the coking value of CTP is as high as 48 pct (as shown in Table III), which indicates that CTP has high content of coking substances and can form plastic mass in the carbonization process. The plastic mass formed by CTP can fully bond the particles and formed a hard carbonized skeleton, which is beneficial to making the structure of ICA dense and improving the compressive strength of the ICA. However, the dense structure of ICA is not conducive to the diffusion of CO_2 gas in the gasification reaction of ICA. Therefore, when the content of CTP is 7 pct, ICA has the highest compressive strength, the lowest reactivity (the reactivity of ICA has been at a high level under the catalysis of metal iron) and the highest post-reaction strength. As the addition amount of CTP exceeds 7 pct, the microstructure of ICA become loose and porous. It is because that the volatile matter content of CTP is as high as 65 pct (as shown in Table III), and the volatilization of volatile matter during the carbonization process will damage the structure of ICA, which results in the decrease of the compressive strength and the improvement of the reactivity of ICA. The conclusion can be drawn from the above analysis results that ICA has denser structure, higher compressive strength, lower reactivity (still at a high level of around 58.7 pct) and higher post-reaction strength when CTP is added by 7 pct. In addition, according to the above analysis, there is a competition between the structural densification due to the plastic mass formed by CTP and the structural decompaction due to the volatilization of volatile matter by CTP. When the amount of CTP added is less than 7 pct, compared with the structural decompaction due to the volatilization of volatile matter by CTP, the influence of structural densification due to the plastic mass formed by CTP plays a dominant role. When the amount of CTP added is more than 7 pct, compared with the structural densification due to the plastic mass formed by CTP, the influence of structural decompaction due to the volatilization of volatile matter by CTP plays a dominant role.

3. *Raman spectra analysis*

The carbon crystallites structure of ICA with different CTP content was analyzed to reveal the evolution mechanism of metallurgical properties of ICA. The Raman spectra and Raman parameters of ICA with different CTP contents are shown in Figure 9. As the amount of CTP added increases from 0 to 11 pct, I_{D1}/I_G is gradually decreased and then increased, while I_G/I_{all} and L_a is gradually increased and then decreased. It indicates that the disorder of carbon crystallites structure inside ICA is gradually reduced and then intensified, and the graphitization degree is improved and then weakened, which can first promote and then reduce the conversion of coals to coke, and first reduce and then improve the activity of carbon inside ICA.[41] The changes of the conversion of coals to coke can first improve and then decrease the compressive strength of ICA. The changes of the activity of carbon can first reduce and then increase the reactivity of ICA.

Table IV. Band Assignments of FTIR Spectra

Section	Wavenumbers (cm^{-1})	Assignments
Hydroxyl 3650 to 3000 cm^{-1}	3625 to 3550	-OH, -NH, $-NH_2$ (stretching)
	3440 to 3100	-OH (phenolic, alcoholic)
	3120 to 3030	Car-H (stretching)
Aliphatic structures 3000 to 2800 cm^{-1}	2960	Asym.RCH_3
	2943 to 2920	Asym.R_2CH_2
	2900 to 2890	R_3CH
	2875	Sym.RCH_3
	2850	Sym.R_2CH_2
	1730	Carboxyl acids
	1637	Conjugated C=O in -COOH
	1610 to 1500	Aromatic C=C
	1458	Asym.CH_3-, CH_2-
	1437	Aromatic C=C
	1258	C-O in aryl ethers
	1222	C-O and OH, phenoxy structures, ethers
	1195 to 1160	C-O phenols, ethers
	1120	C-O in secondary C-OH groups
	1100 to 1073	C-O in primary C-OH
	1059 to 1000	Alkyl ethers, Si-O
Low-wavenumber aromatic structures and ash 900 to 400 cm^{-1}	880 to 750	Aromatic vibration, Car-H
	571,461	Fe-O

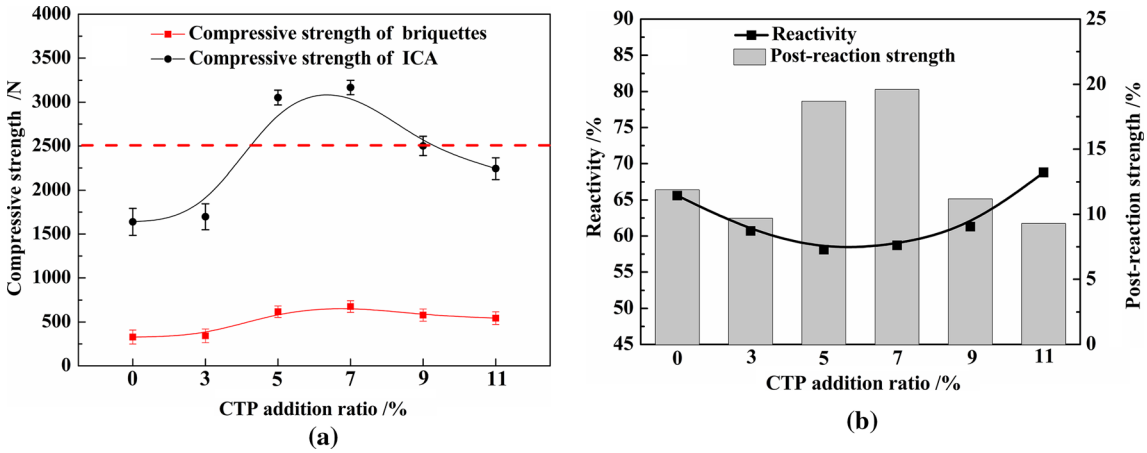

Fig. 7—Evolution of the metallurgical properties of ICA with adding CTP, (*a*) compressive strengths of briquettes and ICA, (*b*) reactivity and post-reaction strength of ICA.

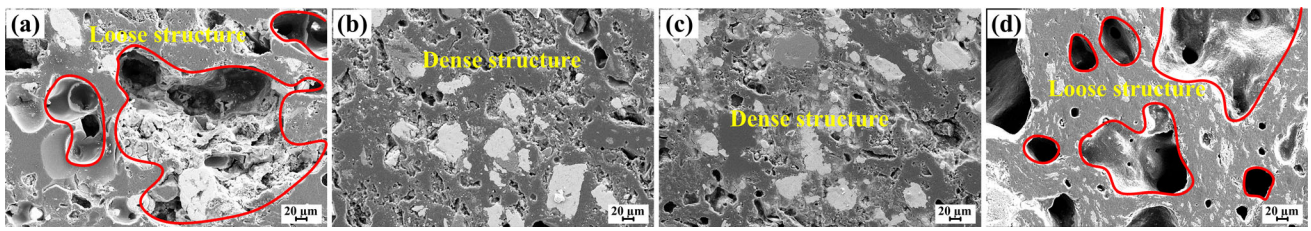

Fig. 8—SEM analysis of ICA with different CTP contents, (*a*) 3 pct, (*b*) 5 pct, (*c*) 7 pct, (*d*) 9 pct.

Therefore, the trend of the degree of regularity in the arrangement of carbon crystallites is consistent with the variation tendency of compressive strength of ICA, but contrary to the change tendency of reactivity of ICA, implying that a higher degree of regularity in the arrangement of carbon crystallites will lead to a lower reactivity of ICA. In addition, the influences of microstructure and activity of carbon on the reactivity of ICA are consistent. Furthermore, the degree of regularity in the arrangement of carbon crystallites is the

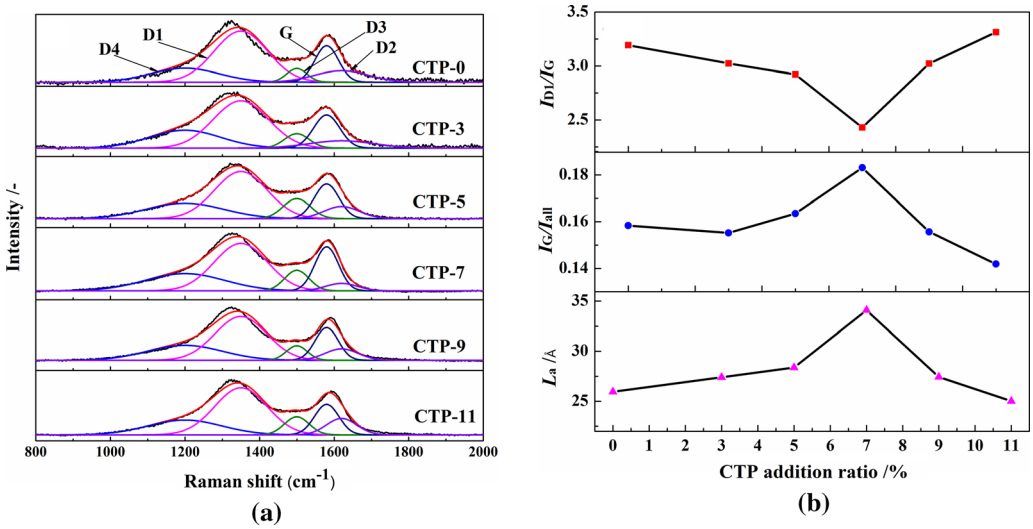

Fig. 9—(*a*) Raman spectra and (*b*) Raman parameters of ICA with different CTP contents.

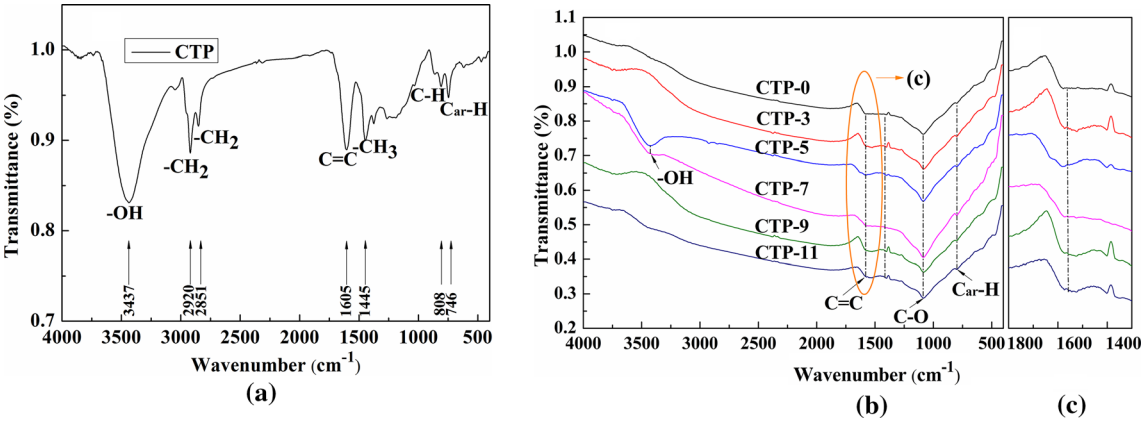

Fig. 10—FTIR spectra of (*a*) CTP, (*b*) ICA with different CTP additions, (*c*) a partial enlarged view of figure (*b*).

highest when the ratio of CTP is 7 pct. Therefore, the compressive strength of ICA is the largest and the reactivity of ICA is relatively lower when the content of CTP is 7 pct.

4. *FTIR analysis*

In order to further reveal the influence of CTP addition on the chemical structures of ICA. The FTIR spectra of raw materials and ICA products were analyzed. Figure 10 (a) presents the FTIR spectrum of CTP,[42,43] the stretching vibrational modes of -OH and -CH_2 groups are mainly observed at 3437, 2920 and 2851 cm^{-1}, and the bands of 1605 and 746 cm^{-1} are observed which are assigned to aromatic C=C and aromatic Car-H, respectively. Comparing the FTIR spectrum of coals and iron ore shown in Figure 6, the functional groups of CTP are very similar to the coals. Therefore, CTP has a high affinity with the coals, which facilitates it to form covalent bonds with coals, and improve the compressive strength of briquettes. Moreover, CTP can be softened and decomposed to form the plastic mass during the carbonization process, which can not only strengthen the structural strength of ICA, but also can be involved in the development of the carbon crystallites structure of ICA. As shown in Figures 10(b) and (c), with the increase of CTP addition, the peak intensity of aromatic C=C group at 1528 cm^{-1} is first decreased and then increased. The content of aromatic C=C group is the lowest when the amount of CTP is 5 to 7 pct. When the amount of CTP is increased from 0 to 7 pct, CTP can condense with toluene, alkane and other small molecules to form macromolecules, so the addition of CTP enhances the continuous condensation of aromatic rings to form polycyclic aromatic hydrocarbons with more benzene rings, and the content of aromatic C=C group in ICA is reduced.[22] Therefore, the carbon crystallites structure of ICA is relatively developed, which can intensify the compressive strength of ICA and reduce the reactivity of ICA. However, as the addition of CTP is further increased to 11 pct, the excess CTP will only form lamellas with fewer aromatic rings, which increase the content of aromatic C=C

group and weaken the carbon crystallites structure of ICA, and the volatilization of excess CTP makes the pore structure of ICA develop. Hence, the compressive strength of ICA is decreased and the reactivity of ICA is increased. For the highly reactive ICA, the addition of CTP is beneficial to improve the mechanical strengths of ICA and reduce the reactivity of ICA. However, the beneficial effects of CTP addition are attenuated when the addition amount of CTP exceeds 7 pct. When the ratio of CTP is 7 pct, the mechanical strength and reactivity of ICA are all at optimal levels. Compared with PVA, CTP is more suitable to be the binder of ICA, and the appropriate ratio of CTP is 7 pct.

IV. CONCLUSIONS

1. With the increase of PVA addition ratio from 0 to 1.0 pct, the compressive strength of briquettes is increased from 417 to 716 N. However, the compressive strength of ICA is reduced from 2854 to 2601 N slightly. The addition of PVA is beneficial to improving the compressive strength of briquettes due to the chemical adsorption between the binder and the material particles, but the addition of PVA is not conducive to improving the compressive strength of ICA due to the poor thermal stability of PVA.
2. PVA has few coking components, which will not affect the carbon crystallites structure and chemical structure of ICA, and the addition of PVA will not have a significant impact on the gasification reactivity of carbon inside ICA. The reactivity of ICA present few changes, which are all at about 60 pct with the increase of PVA addition ratio from 0 to 1.0 pct.
3. As the addition of CTP increases from 0 to 7 pct, the compressive strength of ICA is improved from 1639 to 3168 N due to the formation of plastic mass by CTP during the carbonization process. The reactivity of ICA is reduced from 65.6 to 58.1 pct slightly (It is still at a high level) and the post-reaction strength of ICA is increased from 11.9 to 19.6 pct. This is because the plastic mass produced by CTP can be involved in the development of the carbon crystallites structure of ICA and improve the graphitization degree of ICA, which can reduce the reactivity. However, when the content of CTP is further increased from 7 to 11 pct, the beneficial effects of CTP addition are attenuated.
4. Compared with PVA, CTP is more suitable to be the binder of ICA. The metallurgical properties of ICA are at optimal levels when the ratio of CTP is 7 pct, and the compressive strength, reactivity, and post-reaction strength are 3168 N, 58.1 and 19.6 pct, respectively.

ACKNOWLEDGMENTS

This work was financially supported by the National Natural Science Foundation of China-Liaoning Joint Funds (U1808212), the Fundamental Research Funds of the Central Universities of China (N182504010) and Xingliao Talent Plan (XLYC1902118).

REFERENCES

1. Q. Zhang, Z. Wei, J. Ma, Z. Qiu, and T. Du: *Appl. Therm. Eng.*, 2019, https://doi.org/10.1016/j.applthermaleng.2019.04.04.
2. J. Zhao, H. Zuo, Y. Wang, J. Wang, and Q. Xue: *Ironmak. Steelmak.*, 2019, https://doi.org/10.1080/03019233.2019.1639029.
3. H. Wang, M. Chu, W. Zhao, Z. Liu, and J. Tang: *Metall. Mater. Trans. B*, 2019, vol. 50, pp. 324–36.
4. Z. Zhang, J. Meng, L. Guo, and Z. Guo: *Metall. Mater. Trans. B*, 2016, vol. 47, pp. 467–84.
5. W. Xu, W. Cao, T. Zhu, Y. Li, and B. Wan: *Steel Res. Int.*, 2015, vol. 86, pp. 1063–72.
6. X. Liu, X. Han, H. Cheng, X. Yin, R. Guo, X. Zhao, and Q. Wang: *Metall. Res. Technol.*, 2018, vol. 115, pp. 421–30.
7. M. Natio, A. Okamato, K. Yamaguchi, T. Yamaguchi, and Y. Inoue: *Tetsu-to-Hagané*, 2001, vol. 87, pp. 357–64.
8. M. Naito, A. Okamoto, K. Yamaguchi, T. Yamaguchi, and Y. Inoue: *Nippon Steel Tech. Rep.*, 2006, vol. 94, pp. 103–08.
9. S. Nomura, K. Higuchi, K. Kunitomo, and M. Naito: *ISIJ Int.*, 2010, vol. 50, pp. 1388–95.
10. M. Naito, S. Nomura, and K. Kato: *Tetsu-to-Hagané*, 2010, vol. 96, pp. 201–08.
11. A. Kasai and Y. Matsui: *ISIJ Int.*, 2004, vol. 44, pp. 2073–2078.
12. H. Wang, M. Chu, W. Zhao, R. Wang, Z. Liu, and J. Tang: *Ironmak. Steelmak*, 2016, vol. 43, pp. 571–80.
13. H. Wang, W. Zhao, M. Chu, Z. Liu, J. Tang, and Z. Ying: *Powder Technol.*, 2018, vol. 328, pp. 318–28.
14. H. Wang, M. Chu, J. Bao, D. Han, L. Cao, and W. Zhao: *J. Iron Steel Res.*, 2019, vol. 31, pp. 103–11.
15. T. Anyashiki, H. Fujimoto, T. Yamamoto, T. Sato, H. Matsuno, M. Sato, and K. Takeda: *Tetsu-to-Hagané*, 2015, vol. 101, pp. 515–23.
16. Y. Sekine and H. Fujimoto: *ISIJ Int.*, 2019, vol. 59, pp. 1437–39.
17. P. Venter and N. Naude: *J. S. Afr. I. Min. Metall.*, 2015, vol. 115, pp. 329–33.
18. Y.H. Song, W.J. He, Q.N. Ma, Y.H. Tian, and X.Z. Lan: *Int. J. Coal Prep. Util.*, 2020, vol. 40, pp. 376–88.
19. S.J. Liu, Z.W. Chang, S. Yang, Q. Zhang, S.G. Ju, W.G. Du, R. Ma, Z. Wang, and K.X. Zhang: *Asia-Pac J Chem Eng.*, 2020, https://doi.org/10.1002/apj.2414.
20. Q. Zhong, Y. Yang, T. Jiang, Q. Li, and B. Xu: *Fuel Process. Technol.*, 2016, vol. 148, pp. 12–18.
21. China GB/T 4000-2017: Determination of coke reactivity index (CRI) and coke strength after reaction (CSR).
22. Y. Zhao, Y. Zhang, H. Zhang, Q. Wang, and Y. Guo: *J. Anal. Appl. Pyrol.*, 2015, vol. 112, pp. 290–97.
23. C. Zou, Y. She, and R. Shi: *Fuel Process. Technol.*, 2019, vol. 190, pp. 1–12.
24. K. Alexandrino, Á. Millera, R. Bilbao, and M.U. Alzueta: *Fuel Process. Technol.*, 2018, vol. 179, pp. 369–77.
25. L. Jin, X. Bai, Y. Li, C. Dong, H. Hu, and X. Li: *Fuel Process. Technol.*, 2016, vol. 147, pp. 41–46.
26. M. Pawlyta, J. Rouzaud, and S. Duber: *ScienceDirect.*, 2015, vol. 84, pp. 479–90.
27. R. Morga, I. Jelonek, and K. Kruszewska: *Int. J. Coal Geol.*, 2014, vols. 134–135, pp. 17–23.
28. R. Morga, I. Jelonek, K. Kruszewska, and W. Szulik: *Int. J. Coal Geol.*, 2015, vols. 144–145, pp. 130–37.
29. Z. Gai, R. Zhang, and J. Bi: *Energy & Fuels*, 2017, vol. 31, pp. 3759–67.
30. A. Sadezky, H. Muckenhuber, H. Grothe, R. Niessner, and U. Poschl: *Carbon*, 2005, vol. 43, pp. 1731–42.
31. Y. Zhu, X. Zhao, J. Cheng, J. Lu, and S. Lai: *Spectrosc. Spect. Anal.*, 2017, vol. 37, pp. 1919–24.
32. B. Bai, Q. Guo, Y. Li, X. Hu, and J. Ma: *Energy & Fuels*, 2018, vol. 32, pp. 3356–67.
33. S. Moraes, J. De Lima, J. Neto, C. Fredericci, and E. Saccoccio: *Min. Proc. Ext. Met. Rev.*, 2019, https://doi.org/10.1080/08827508.2019.1604521.

34. K. Zhang, Y. He, Z. Wang, T. Huang, Q. Li, S. Kumar, and K. Cen: *Fuel*, 2017, vol. 210, pp. 738–47.
35. F. Meng, J. Yu, A. Tahmasebi, Y. Han, H. Zhao, J. Lucas, and T. Wall: *Energy & Fuels*, 2014, vol. 28, pp. 275–84.
36. S. Patra, A. Pattanaik, and V. Rayasam: *Can. Metall. Quart.*, 2019, vol. 58, pp. 28–45.
37. J. Cai, S. Yang, X. Hu, W. Song, Q. Xu, B. Zhou, and Y. Song: *Fuel*, 2019, vol. 253, pp. 339–48.
38. Z. Shi, L. Jin, Y. Zhou, Y. Li, and H. Hu: *Fuel Process. Technol.*, 2017, vol. 167, pp. 648–54.
39. S. Qiu, S. Zhang, Y. Wu, G. Qiu, C. Sun, Q. Zhang, J. Dang, L. Wen, M. Hu, J. Xu, R. Zhu, and C. Bai: *Fuel*, 2018, vol. 232, pp. 374–83.
40. K. Naveen Kumar, R. Padma, L. Vijayalakshmi, and J. Maria Nithya: *J. Lumin.*, 2017, vol. 182, pp. 208–19.
41. Sushil. Gupta, Veena. Sahajwalla, Jonathan. Burgo, Pinakin. Chaubal, and Ted. Youmans: *Metall. Mater. Trans. B*, 2005, vol. 36, pp. 385–94.
42. S. Sun, L. Wang, C. Wang, and Y. Zhang: *Vacuum.*, 2018, vol. 158, pp. 215–17.
43. Y. Feng, Y. Wang, G. Liu, J. Shen, R. Li, J. Du, Z. Yang, and Q. Xu: *J. Clean. Prod.*, 2018, vol. 172, pp. 2544–52.